An Approach to Elongated Fine-Particle Magnets

I. S. JACOBS AND C. P. BEAN
General Electric Research Laboratory, Schenectady, New York
(Received June 21, 1955)

The coercive force predicted by theory for single-domain particles with shape anisotropy frequently far exceeds the observed value. From an examination of the results of Paine, Mendelsohn, and Luborsky on elongated iron particles, several approximate models are suggested which may exist in certain experimental situations. Detailed calculations are presented for a "chain-of-spheres" model remagnetizing by several mechanisms. Comparison with experiment on certain single-domain particles of known elongation favors the chain-of-spheres model as a suitable description of their magnetic behavior. A successful calculation is made of the coercive force of material prepared by several earlier workers. A comparison of the new models with the older ones indicates a direction for experimental advance.

INTRODUCTION

SINCE the suggestion of Frenkel and Dorfman[1] in 1930, there has been active interest in the magnetic properties of particles small enough, on energetic grounds, to contain but one domain when there is no applied magnetic field. The theory describing such single-domain particles has been enlarged by Guillaud,[2] Néel,[3] Kittel,[4] Stoner and Wohlfarth,[5] and Kondorskii.[6] Thorough expositions of this field may be found in the survey by Kittel[7] and in the work of Stoner and Wohlfarth,[5] with much experimental work appearing in the reports of recent conferences on magnetism.[8,9]

The coercive force of a single-domain particle is generally expected to have a high value, since the magnetization changes occur, as a limiting case, through the usually high field process of rotation of the total magnetic moment of the particle. This rotation process is controlled by the effective anisotropy of the particle, for which a number of sources are usually considered.[7] The present paper is concerned with the coercive force of fine particles, resulting from anisotropy of particle shape. If the particle has the shape of a prolate spheroid whose major axis coincides with the field direction, its intrinsic coercive force is given by $H_c=(N_t-N_0)I_s$, where I_s is the saturation magnetization, and N_0, N_t are the demagnetizing factors of the spheroid along the major and minor axes, respectively. Stoner and Wohlfarth have presented a very detailed treatment of this process, including the averaging for random orientation of particle axes. This mechanism is probably operative in certain heterogeneous alloys[5,10,11] and it probably contributes to the coercive force of some fine particles produced by reduction or electrodeposition of ferromagnetic materials.[3,12–15]

The realization of the predicted magnetic properties for elongated single-domain particles has been hindered by experimental difficulties. On the theoretical side, there exists the possibility of finding a mechanism for magnetization reversal with lower energy than the Stoner and Wohlfarth mechanism of simultaneous parallel rotation of all the atomic moments.[16,17] In a current paper,[18] Paine, Mendelsohn, and Luborsky demonstrate the predominance of a shape-anisotropy effect on the coercive force of elongated single-domain particles of iron produced during electrodeposition. Dilute suspensions of this material have coercive forces as high as 2000 oe. Observations in an electron microscope reveal the anisotropy of shape of these particles and an average particle diameter of 150 A. Such electron micrographs enable the preparation of particle elongation distribution curves for each sample. This information makes possible a comparison of fine-particle theory with single-domain particles of known elongation. An ideal situation of this kind has seldom, if ever, been realized in fine-particle work.

It is instructive to make a rough comparison of the elongated fine-particle iron described by Paine *et al.* with the predictions of the Stoner-Wohlfarth analysis. Theoretically, two situations are of interest, that of perfect alignment and that of complete randomness in the orientation of the elongated particles. Experimentally, this material is capable of a partial alignment with some resulting directionality in magnetic properties. For the present we neglect crystal anisotropy and use the median elongation to characterize the assembly. For dilute suspensions with a median elongation of 3 to 1 (Samples *B* and *C* of reference 18), a representative

[1] J. Frenkel and J. Dorfman, Nature **126**, 274 (1930).
[2] C. Guillaud, Revs. Modern Phys. **25**, 308 (1953).
[3] L. Néel, Compt. rend. **224**, 1488, 1550 (1947).
[4] C. Kittel, Phys. Rev. **70**, 965 (1946).
[5] E. C. Stoner and E. P. Wohlfarth, Trans. Roy. Soc. (London) **A240**, 599 (1948).
[6] E. Kondorskii, Doklady Akad. Nauk. S.S.S.R. **70**, 215 (1950).
[7] C. Kittel, Revs. Modern Phys. **21**, 541 (1949).
[8] Revs. Modern Phys. **25**, 1–351 (1953).
[9] J. phys. radium **12**, 151–508 (1951).
[10] L. Néel, Compt. rend. **225**, 109 (1947); Appl. Sci. Research **B4**, 13 (1954).
[11] Nesbitt, Williams, and Bozorth, J. Appl. Phys. **25**, 1014 (1954); E. A. Nesbitt and R. D. Heidenreich, J. Appl. Phys. **23**, 366 (1952).
[12] L. Weil, J. phys. radium **12**, 437 (1951).
[13] J. K. Galt, Phys. Rev. **77**, 845 (1950).
[14] A. Mayer and E. Vogt, Z. Naturforsch. **7a**, 334 (1952).
[15] W. H. Meiklejohn, Revs. Modern Phys. **25**, 302 (1953).
[16] L. J. Dijkstra, *Thermodynamics in Physical Metallurgy* (American Society for Metals, Cleveland, 1950), p. 271.
[17] C. P. Bean (unpublished).
[18] Paine, Mendelsohn, and Luborsky, this issue [Phys. Rev. **100**, 1055 (1955)].

coercive force when in the random arrangement is about 1500 oe (measured at −196°C). Alignment may raise this to 1700 or 1800 oe in the parallel direction by about 1200 to 1400 oe in the transverse direction. The Stoner-Wohlfarth calculations predict about 3500 oe for the random-state coercive force and 7200 oe by 0 oe for the aligned state. This discrepancy warrants further attention. In what follows, there will be described a simple model with several variations which is capable of accounting for a number of experimental observations made on this elongated fine-particle iron.

"CHAIN-OF-SPHERES" MODEL

An alternative model of an elongated particle is a chain of single-domain spheres, rather than the prolate ellipsoid employed by Stoner and Wohlfarth. In this idealized model the spheres are sometimes assumed to have only point contact, or even to be slightly separated so as to be magnetically isolated. We shall refer to this model as a "chain of spheres."

This sort of model has been envisaged in the past,[19,20] and suggestions have been made for obtaining the chain experimentally. Beischer and Winkel[20] have noted a self-alignment feature in the model and presented some experimental evidence for it. Briefly stated, the self-alignment mechanism is that single-domain spheres have a tendency to line up with their moments along the common axis, due to magnetostatic interactions. To consider the alignment mechanism, we treat each sphere as a dipole of moment μ and diameter a, and examine their interactions. If dipoles μ_i and μ_j, separated by a distance r_{ij}, make angles θ_i and θ_j with the vector joining them, their energy is

$$W=(\mu_i\mu_j/r_{ij}^3)[\cos(\theta_i-\theta_j)-3\cos\theta_i\cos\theta_j]. \quad (1)$$

Adding terms of this type, it is easy to show that two spheres in contact are most stable with their moments aligned along the line of centers. Similarly, for three spheres the aligned configuration is more stable than any other, including those which offer a sort of flux closure. This situation changes when we allow four spheres to come together. Now, the flux closure configuration of a square array, moments at 45° to connecting lines, is more stable than the aligned configuration. The self-alignment mechanism need not fail at this point, however, for if a fourth sphere approaches a straight chain of three, its most stable position is at the chain end, provided we admit no mechanism for deforming the chain. With this growth feature, aided by some unspecified welding of spheres, this scheme may be added to those previously considered for making connective chains.

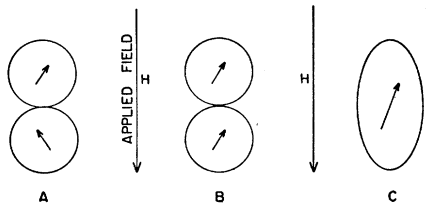

FIG. 1. Magnetization reversal of aligned chain or particle. Chain-of-spheres model: *A*—symmetric fanning mechanism; *B*—parallel rotation mechanism. Prolate spheroid model: *C*—parallel rotation mechanism.

COERCIVE FORCE OF ALIGNED CHAINS

The principal object of this paper is the calculation of the coercive force of dilute suspensions, using the chain-of-spheres model. We shall be concerned first with the coercive force when the chain is aligned with the field. This will be followed by the appropriate averaging over all orientations of the chain with respect to the field, so as to obtain the coercive force for an assembly of randomly oriented chains. At that point we may compare the predictions of the model with experiment.

For the calculation, we assume that the spheres have no crystal anisotropy. The shape anisotropy of the chains will follow from the arrangement of the dipolar spheres as they interact with each other and with the external field. There are two reversal mechanisms which will be considered for the chain of spheres. (See Fig. 1.) The simpler one is that of simultaneous parallel rotation of each of the dipole moments in the chain. (This will be designated as mechanism *B*.) This mechanism is identical to that employed by Stoner and Wohlfarth, with the exception that the specific value for the coercive force of a chain proves to be lower than that for an ellipsoid of the same axial ratio. The averaging procedure is identical, yielding the same numerical factor (0.479) relating the coercive force of the randomly oriented assembly to that of the perfectly aligned (noninteracting) assembly. The second mechanism is that in which the moments fan out in a plane, alternating in the sense of their rotation from one sphere to the next, proceeding along the chain. We assume here that there is no exchange-energy interaction where adjacent spheres are closest. In other words, the "wall" area is confined to the "point" of contact, or the spheres are slightly separated. It is easy to show that fanning in a plane is favored over any other arrangement of fanning with respect to the chain axis. A special case of this observation is that the mechanism of fanning in a plane yields a lower magnetostatic energy during magnetization reversal than does the simultaneous parallel-rotation mechanism. It is instructive, however, to include the calculations for the higher-energy process, as it may occur if the wall energy contribution becomes significant. It is important to note that a simplifying assumption is made in the calculations for the fanning mechanism, i.e., the magnitude of the angle of fanning is constant along the length of the chain. This assumption of symmetric fanning is rigorously correct for the two-sphere chain and for the infinitely long chain whose

[19] U. S. Materials Advisory Board, Panel on Permanent Magnet Materials, Report MMAB-34-M, 1953 (unpublished).
[20] D. Beischer and A. Winkel, Naturwiss. 25, 420 (1937).

ends meet. Separate calculations of the coercive force, made without the above restriction, for aligned chains of finite and semi-infinite length show the existence of an end effect. This leads to lower coercive forces than those predicted by symmetric fanning. Exact solutions are readily obtained for aligned chains of six or less spheres. For the semi-infinite chain a close approximation is obtained by starting with a trial solution suggested by a soluble model involving only nearest neighbor interactions. When considering the reversal by fanning of unaligned chains, the symmetric-fanning model is more tractable. Consequently this mechanism will be retained for detailed investigation. It will be shown that the errors originating in its use are small when the chains are not long. (We shall designate the symmetric-fanning process as A and the nonsymmetric-fanning process as A'.)

To calculate the coercive force for a chain aligned with the field, we consider the total energy of the chain at some point during the reversal, being the sum of the interdipole magnetostatic energy and the field energy with the field directed opposite to the initial direction of magnetization of the chain. This energy is minimized with respect to its angle parameter to obtain an expression for the equilibrium field for a given angle. The coercive force is obtained from this expression by inspection. In the case of parallel rotation, $\theta_i=\theta_j=\theta$ for all i, j in the chain of n. The total energy is then

$$W_n=(\mu^2/a^3)nK_n(1-3\cos^2\theta)+n\mu H\cos\theta, \quad (2)$$

where

$$K_n=\sum_{j=1}^{n}(n-j)/nj^3. \quad (3)$$

Proceeding as described, the coercive force for parallel rotation, B, is

$$H_{c,n}=(\mu/a^3)6K_n. \quad (4)$$

In similar fashion, for the symmetric fanning mechanism where $\theta=\theta_1=-\theta_2=\theta_3=-\theta_4=\cdots$, we write for the total energy:

$$W_n=(\mu^2/a^3)nL_n(\cos2\theta-3\cos^2\theta)+(\mu^2/a^3)nM_n(1-3\cos^2\theta)+n\mu H\cos\theta, \quad (5)$$

where

$$L_n=\sum_{j=1}^{\frac{1}{2}(n-1)<j\leq\frac{1}{2}(n+1)}[n-(2j-1)]/n(2j-1)^3, \quad (6)$$

$$M_n=\sum_{j=1}^{\frac{1}{2}(n-2)<j\leq\frac{1}{2}n}(n-2j)/n(2j)^3, \quad (7)$$

$$L_n+M_n=K_n. \quad (8)$$

Thus we obtain for the coercive force in the fanning mechanism, A,

$$H_{c,n}=(\mu/a^3)(6K_n-4L_n). \quad (9)$$

Noting that $\mu/a^3=\pi I_s/6$ which is about 900 oe for iron, we may tabulate the coercive forces for chains (or elongated particles) of various lengths (or axial ratios). This is done in Table I, and includes the results for the nonsymmetric fanning mechanism, A', along with the coercive forces for prolate spheroids, C, calculated as indicated previously.

TABLE I. Comparison of coercive force of chains or particles of iron aligned with magnetic field. (A) Chain of n, symmetric fanning mechanism Eq. (9). (A') Chain of n, nonsymmetric fanning mechanism. (B) Chain of n, parallel rotation mechanism, Eq. (4). (C) Prolate spheroid of axial ratio n, parallel rotation mechanism.

n Chain length or axial ratio	H_c in oersteds A	A'	B	C
1	0	0	0	0
2	900	900	2700	5160
3	1420	1400	3820	7260
4	1690	1590	4430	8340
5	1870	1680	4810	8980
6	2020	1720	5070	9400
7	2090	···	5260	9650
8	2160	···	5390	9860
9	2220	···	5530	10 000
10	2270	···	5630	10 100
11	2310	···	5700	10 200
12	2340	···	5760	10 300
∞	2700	1750	6470	10 800

Several points are of interest in connection with the data of Table I. As implied above, the fanning mechanisms (A,A') have lower coercive forces than the other mechanisms. For experiments with elongated particles, it is particularly significant that the maximum coercive forces by fanning are considerably lower than the corresponding maximum attainable with parallel rotation of the magnetic moments in an ellipsoid (C). The lower coercive forces of the various chain models compare attractively with existing experimental results.

MAGNETIZATION OF RANDOMLY ORIENTED CHAINS

We have now to obtain the hysteresis loop for an assembly of randomly oriented chains of spheres, when the magnetization reversal mechanism of a chain aligned with the field is the symmetric-fanning process, A. For mechanism A', we shall use an approximation based on A, while B is similar to C, previously described.[5] The composite loop is synthesized from the family of loops corresponding to different angles between the field and the chain axis. As this angle approaches 90°, the reversal mechanism will change over to that of simultaneous parallel rotation. This feature is responsible for an approximate equivalence of the random and aligned coercive forces. There is no universal random loop, adjustable to chain length by a scale factor, because the ratio K_n/L_n, Eq. (9), is a slowly varying function of n. We carry out specific calculations for two cases, a chain of two spheres and an infinitely long chain, and interpolate for chains of intermediate length.

The choice of coordinates facilitates the calculation. Consider that the field, H, is applied along the z-axis,

in the $-z$-direction. Let the chain lie in the xz-plane, its axis making an angle ψ with the z-axis. The sphere moments will be described by their polar angle θ, with respect to the z-axis, and their azimuthal angle ϕ measured in the xy-plane, with respect to the x-axis. During the fanning process, the angle ϕ alternates in sign from one sphere to the next along the chain, but $|\phi|$ is constant in accordance with our assumption for this process, A. In terms of this description, the total energy for a chain of n spheres, comprised of magnetostatic and field energy terms, is given by

$$\begin{aligned} W_t(\theta,\phi,\psi,H) &= W_{ms}(\theta,\phi,\psi)+W_f(\theta,H) \\ &= -3nK_n(\mu^2/a^3)(\sin\psi\sin\theta\cos\phi \\ &\quad +\cos\psi\cos\theta)^2+nL_n(\mu^2/a^3)(\sin^2\theta\cos 2\phi \\ &\quad +\cos^2\theta)+nM_n(\mu^2/a^3)+n\mu H\cos\theta, \end{aligned} \tag{10}$$

where K_n, L_n, and M_n are given by Eqs. (3), (6), and (7). To determine the hysteresis loop for a chain making a given angle ψ with the field, we calculate the equilibrium values of θ and ϕ at various values of the field H, i.e., minimize W_t at fixed ψ, H. The loop is then formed by plotting the resolved relative magnetization $I/I_s=\cos\theta$ *versus* H. The equations to be solved simultaneously are

$$(\partial W_t/\partial\phi)_\theta=(\partial W_{ms}/\partial\phi)_\theta=0, \tag{11}$$

$$(\partial W_t/\partial\theta)_\phi=(\partial W_{ms}/\partial\theta)_\phi+dW_f/d\theta=0. \tag{12}$$

From Eq. (11) we obtain a relation between θ and ϕ, which, upon substitution into Eq. (12), yields an equation in θ alone, depending on ψ and H as parameters. We complete the solution for θ graphically, by fixing ψ, plotting $(\partial W_{ms}/\partial\theta)_\phi$ and $-(dW_f/d\theta)$ for a given H, and determining their intersection. A simplification is introduced by using $\sin\theta$ as abscissa, in which case $(dW_f/d\theta)$ is a straight line whose slope is proportional to H.

To describe the features of the reversal, we first examine the roots of Eq. (11), which are

$$\sin\phi=0, \quad \phi=0,\pi \tag{13}$$

and

$$\cos\phi=A(\psi)\cot\theta, \tag{14}$$

where

$$A(\psi)=(3K_n/4L_n)\sin 2\psi/[1-(3K_n/2L_n)\sin^2\psi]. \tag{15}$$

The first of these indicates parallel rotation of the moments, leading to the results of Stoner and Wohlfarth. The correct choice for our model is obtained by invoking a necessary condition for a minimum, i.e., $(\partial^2 W_t/\partial\phi^2)_\theta>0$. This condition is satisfied as follows:

(a) by $\phi=0$, for $0\leq\theta<\tan^{-1}A(\psi)$;

(b) by $\phi=\cos^{-1}[A(\psi)\cot\theta]$, for $|\tan\theta|\geq A(\psi)$;

(c) by $\phi=\pi$, for $\cot^{-1}(-1/A(\psi))<\theta\leq\pi$.

The reversal mechanism is some sort of fanning in range (b), but this range becomes smaller as ψ increases

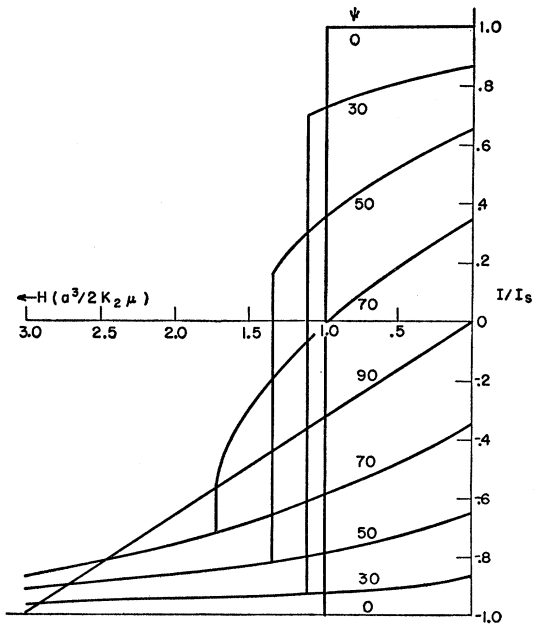

FIG. 2. Hysteresis loops for two-sphere chains oriented at various angles ψ to field. (Fanning mechanism.)

until $\psi\geq\psi_0=\sin^{-1}(2L_n/3K_n)^{\frac{1}{2}}$ for which there is no longer a solution to Eq. (14). The angle ψ_0 varies from 54.8° for $n=2$ to 49.8° for $n=\infty$. For $\psi\geq\psi_0$, the complete reversal is by the parallel-rotation mechanism. The polar angle $\theta=\tan^{-1}A(\psi)$, marking the transition from parallel-rotation reversal to fanning reversal, increases with increasing ψ until $\psi=\psi_0$, at which point $\theta(\psi_0)=\pi/2$. Other features of the reversal appear in the graphical solution. For $\psi<\psi_0$, as H increases, there is a gradual change in $\cos\theta$, followed by a discontinuous change just at the angle θ marking the transition from parallel to fanning reversal. The only stable solutions occur in ranges (a) and (c), while range (b) is needed to permit the discontinuous reversals at fields lower than would occur with the parallel rotation mechanism alone. These fields mark the coercive forces for the loops in question. For $\psi\geq\psi_0$, discontinuous changes occur at $H>H_c$, as described by Stoner and Wohlfarth.

The results, in the form of graphs of representative hysteresis loops, are shown in Figs. 2 and 3 for $n=2$ and $n=\infty$, respectively. In Fig. 4, showing H_c *versus* ψ for mechanisms A and B, it is interesting to note the gradual rise in H_c (fanning) from its value at $\psi=0$, until it meets H_c (parallel rotation) at $\psi=\psi_0$ and then falls rapidly to zero. This comparison demonstrates the large difference between mechanisms A and B in their numerical "averaging" factor relating the aligned coercive force to that for a randomly oriented assembly.

Using data calculated for loops of constant ψ in 10° intervals, we proceed to the synthesis of the loops for an assembly of randomly oriented chains, all having either $n=2$ or $n=\infty$. The mean resolved value of the relative magnetization of the assembly at a particular

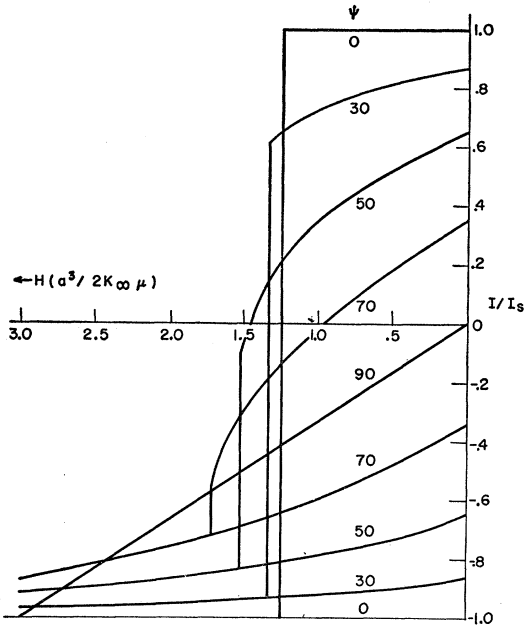

FIG. 3. Hysteresis loops for ∞-sphere chains oriented at various angles ψ to field (symmetric fanning mechanism).

field H is given by

$$\langle (I/I_s)_H \rangle_{Av} = \langle (\cos\theta)_H \rangle_{Av} = \int_0^{\pi/2} (\cos\theta)_H \sin\psi d\psi, \quad (16)$$

where the value of θ may depend on the previous history. In performing the graphical integration, integrand discontinuities lead to uncertainty in some of the points, but the resulting curves are sufficiently accurate for present purposes. The curves for $n=2$ and $n=\infty$ are shown in Figs. 5 and 6, while Table II presents data from which these curves may be reproduced. The most important results are the values of the random coercive force, as follows:

Chain length $n=2$;

$$\bar{H}_c = (1.13 \pm 0.02)(2K_2\mu/a^3) = 1.13 H_c(\psi=0),$$

Chain length $n=\infty$;

$$\bar{H}_c = (1.35 \pm 0.03)(2K_\infty\mu/a^3) = 1.08 H_c(\psi=0).$$

These findings are novel, in that the random coercive force exceeds the aligned coercive force, but, in practice, a number of factors may tend to mask this effect.

Figure 7 presents a comparative summary and evaluation of the results for the field of fine-particle ferromagnetic material having shape anisotropy. Specifically considered are the hysteresis loops for random and aligned assemblies reversing by three mechanisms,

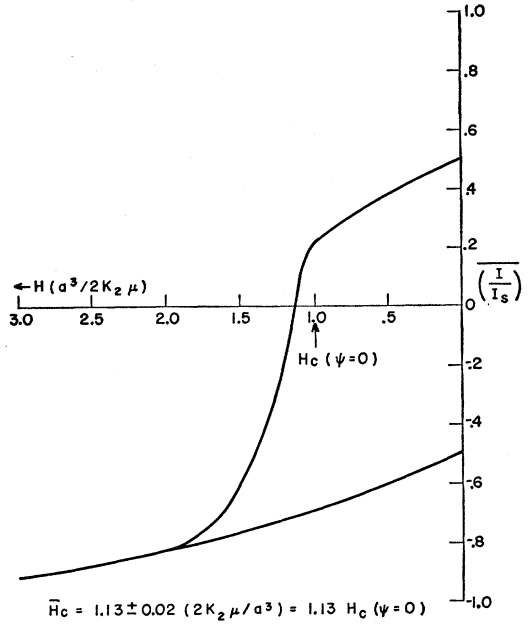

FIG. 5. Hysteresis loop of assembly of randomly oriented two-sphere chains. (Fanning mechanism.)

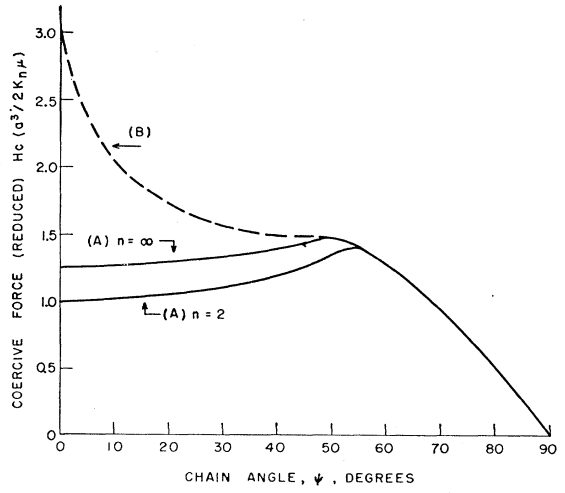

FIG. 4. Variation of coercive force with angle ψ between chain and field. (A) Symmetric fanning mechanism; $n=2$, $n=\infty$. (B) Parallel-rotation mechanism, all n.

fanning (A) and parallel rotation (B) for chains of spheres, and parallel rotation (C) for prolate spheroids. Curves A describe the magnetic behavior when the spheres of the chain appear isolated to the extent of feeling no exchange forces, but are subject to strong magnetostatic interaction. Curves B pertain when there is sufficient common boundary between the spheres of the chain to allow a strong exchange interaction which forces the reversal mechanism to be parallel rotation. This interaction raises the random coercive force but slightly, while the aligned coercive force increases by a factor of three over that in A. Curves C show a twofold increase in both coercive forces over those in B, illustrating the improvement in magnetic properties to be obtained when the chain is "filled out" to become a prolate spheroid. From the theoretical

side, there are three idealized models for analysis of actual situations which may be close to one of them, or lie between two of them.

COMPARISON WITH EXPERIMENT

The particle elongation distribution curves presented by Paine, Mendelsohn, and Luborsky[18] enable us to compare the magnetic properties predicted by the various models with their results. For the chain-of-spheres model, only integral elongation ratios are allowed, so unit length is assigned to particles whose ratios lie between 1 and 1.5, length 2 to particles between 1.5 and 2.5, and so on. This information is converted to histograms showing the volume percentage of particles in each group. The existence of universal hysteresis loops for mechanisms B and C facilitates

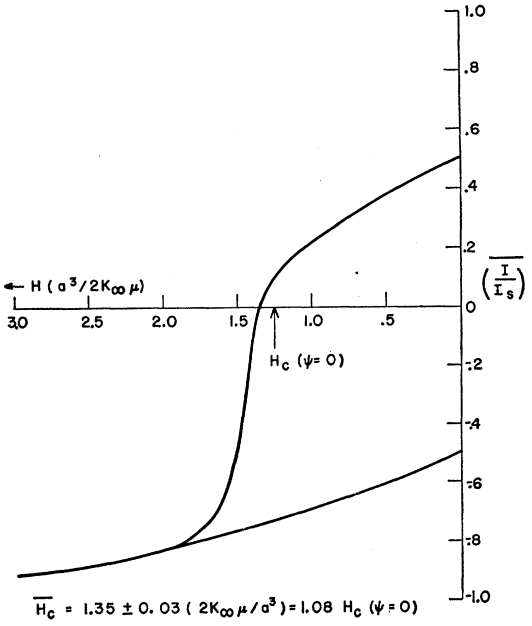

FIG. 6. Hysteresis loop of assembly of randomly oriented ∞-sphere chains (symmetric fanning mechanism).

the application of these data following the procedure recently described by Wohlfarth.[21] His integration is replaced here by a summation. When calculating the random coercive force for the symmetric fanning mechanism (A), the variation with n of the reduced hysteresis loops, Figs. 5 and 6, introduces a little more work. The required interpolation for intermediate values of n is done in a straightforward manner, and the results are relatively insensitive to the exact method employed. For the nonsymmetric fanning mechanism (A'), only an approximate calculation of coercive force can be made, in the absence of a detailed hysteresis loop for a randomly oriented assembly. One simple approximation is to use the loop for a chain of two

[21] E. P. Wohlfarth, Research (London) 7, S1 (1954).

TABLE II. Variation of relative magnetization with field for a randomly oriented assembly of n-sphere chains; $n=2$, $n=\infty$ (symmetric fanning mechanism).

$Ha^3/\mu 2K_n$	Upper branch (I/I_s) $n=2$, $n=\infty$		Lower branch (I/I_s) $n=2$, $n=\infty$
0.0	+0.500[a]		−0.500[a]
0.2	+0.453		−0.542
0.4	+0.402		−0.582
0.6	+0.349		−0.620
0.8	+0.288		−0.655
1.0	+0.220±0.002		−0.687
1.2	−0.195±0.005	+0.140±0.002	−0.718
1.4	−0.495±0.005	−0.150±0.050	−0.747
1.6	−0.675±0.005		−0.774
1.8	−0.775±0.005		−0.799
2.0	−0.822±0.002		−0.822
2.2	−0.840±0.002		−0.841
2.4	−0.862		−0.864
2.6	−0.884		−0.884
2.8	−0.898		−0.898
3.0	−0.913		−0.913
3.5	−0.938		−0.938
4.0	−0.957		−0.957
5.0	−0.972		−0.972
6.0	−0.981		−0.981

[a] The data listed without error limits were interpolated from Stoner and Wohlfarth (reference 5), Table VI. The graphical solution is accurate to ±0.002 except as noted.

spheres, applying a suitable scaling factor based on the aligned coercive forces of Table I.

Calculations of the coercive force were made with the various models for two rather different dilute samples. The first of these, designated $S-C$ (about the same as sample C of reference 18), is typical of those for which the chain-of-spheres model was devel-

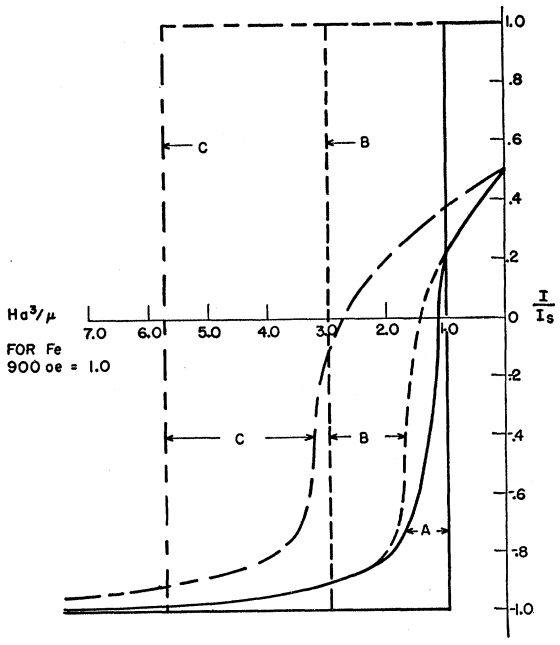

FIG. 7. Comparison of hysteresis loops for assemblies of randomly oriented and aligned two-sphere chains; three reversal mechanisms. A—fanning; B—parallel rotation of sphere moments; C—parallel-moment rotation in spheroid of axial ratio 2:1.

TABLE III. Summary of coercive force calculations. Samples described by Paine *et al.*[a] Mechanisms of reversal: *A*—chain of spheres, symmetric fanning; *B*—chain of spheres, parallel rotation; *C*—prolate spheroids, parallel rotation. Combinations use *C* for elongations <1.5.

Sample	*S*−*C*		*S*−*A*	
Observed $H_{c\parallel}=H_{c\perp}$	1500 oe		1100 oe	
Model	H_c Random[b] oe	H_c Aligned oe	H_c Random[a] oe	H_c Aligned oe
A	1590	1690	420	900
B	1750	4430	400	2700
C	3280	8340	1250	5160
A+*C*	1610	1700	970	1420
B+*C*	1750	4430	980	2700

[a] Reference 18.
[b] The error in the calculational procedure is estimated as ±20 oe.

oped. Its particles have a mean diameter of about 150 A, and a median elongation ratio of about 3, with contributions from particles having axial ratios up to 13. The second sample, *S*−*A* (about the same as sample *A* of reference 18), was prepared under different conditions and is less suited to the chain-of-spheres model. This sample is similar in its magnetic and particle-shape properties to material investigated by Meiklejohn[15] and by Mayer and Vogt.[14] Its particles have the same mean diameter of 150 A, but they exhibit very little elongation, the median being 1.3 to 1 with the largest about 5 to 1. As this sample has an important fraction of its volume in the range of elongation between 1.0 and 1.5, the arbitrary criterion above, which assigned unit length and zero coercive force to this range, should be modified. A useful approximation is to treat them as prolate spheroids of axial ratio 1.25. This is done below for mechanism *C* in which all particles are considered as Stoner-Wohlfarth spheroids. This approximation may also be combined with reversal mechanisms *A* and *B* for the chains of spheres. When the fraction of material in this low elongation group is small, the use of such a combination is unimportant.

Table III presents the results of such calculations, along with the experimentally observed coercive forces at −196°C, in directions parallel and perpendicular to that of the field during solidification of the matrix. These samples showed no tendency to directionalize while many others did. Coercive force estimates for aligned samples are included, as they will prove useful in discussing samples which do exhibit directional effects. In connection with Table III, we shall note errors and omissions made along the way. The error of about ±20 oe stated for H_c (random) represents only an estimate of the error in the calculational procedure. The results of the approximate calculations for these samples using the nonsymmetric-fanning mechanism, *A'*, are not listed as they fall within the error limits. A significant error from this source does not appear until the median elongation ratio is about five or greater. An important omission is the effect of magnetocrystalline anisotropy. This could add to the calculated coercive force an amount varying from $2K/I_s$ to $-2K/I_s$ depending on the degree of crystalline order along the chain. For iron at −196°C, the higher estimate amounts to about 600 oe.

On the basis of the evidence up to this point, sample *S*−*C* seems best described by mechanism *A*, although we cannot reject mechanism *B*. This agreement with the chain-of-spheres model is not surprising inasmuch as this sample exhibits a symmetrically wavy profile along the sides of its elongated particles. (See Figs. 2 and 3 of reference 18.) With regard to sample *S*−*A*, the agreement with experiment of either of the two combination models is gratifying. The prolate spheroid model *C*, also gives reasonable results for this sample. These estimates for *S*−*A* have a more quantitative basis than previous estimates for this type of sample.[3,12,21]

In recent work, Paine and co-workers[22] have investigated the effect, on the coercive forces, of the magnitude of the aligning field during freezing of the matrix. Measurements on a sample similar to *S*−*C*, in directions parallel and perpendicular to the direction of the freezing field, show a small increase in $H_{c\parallel}$ and a rather

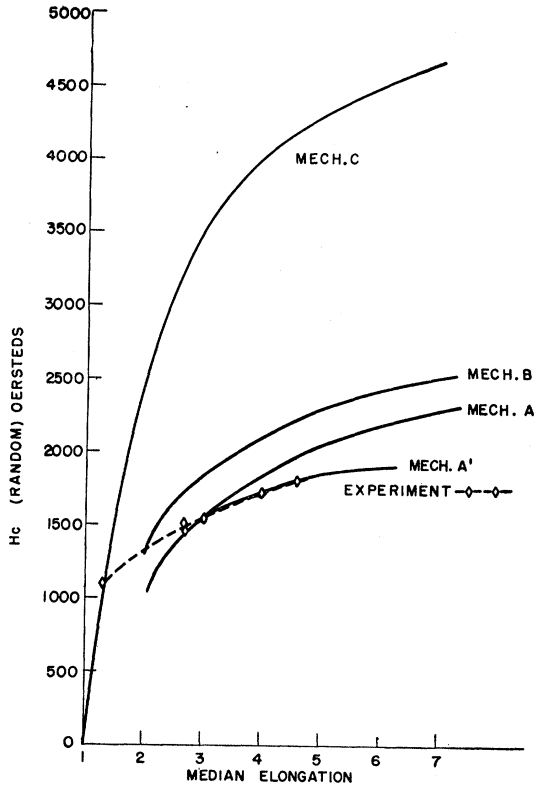

FIG. 8. Comparison of observed and calculated values of random coercive force of fine particle iron as a function of median elongation. Chain-of-spheres model: *A*—symmetric fanning mechanism; *A'*—nonsymmetric-fanning mechanism; *B*—parallel-rotation mechanism. Prolate spheroid model: *C*—parallel-rotation mechanism.

[22] Paine, Mendelsohn, and Luborsky (private communication).

larger decrease in $H_{c\perp}$. The magnitude of the decrease is more than twice that of the increase. This asymmetrical spread resembles the behavior expected from mechanism A. For the completely aligned state, each mechanism predicts $H_{c\perp}\approx 0$, but for mechanism A, $H_{c\parallel}\approx \bar{H}_c$, as compared to the predictions for mechanisms B and C of $H_{c\parallel}\approx 2\bar{H}_c$.

An additional comparison between theory and experiment may be made with the relation between random coercive force and median elongation ratio. Data have been collected[18,22] for samples ranging in median elongation ratio (by frequency) from 1.3 to 4.6, with particle diameters lying between 140 A and 180 A. For the models, we assume that the median elongation adequately characterizes the behavior, and we determine the random coercive force of a sample of uniformly elongated particles (neglecting magnetocrystalline anisotropy). Figure 8 presents the comparison of experiment with mechanisms A, A', B, and C. Mechanism C is ruled out at high elongation, as noted earlier. The failure of models A, A', and B at low elongation is also as expected. The general trend of predictions A, A', and B is in fair agreement with the experimental results at higher elongations. In particular, despite the crudeness of the assumptions, there is apparent support for the fanning mechanism A' in this correlation.

SUMMARY

We have re-examined the predictions of magnetic behavior arising from shape anisotropy in single-domain particles. Several approximate models have been suggested which may exist in certain experimental situations. Detailed calculations have been carried out for a "chain-of-spheres" model. Comparison with recent results on certain elongated iron particles favors the chain-of-spheres model as a suitable description of their magnetic behavior. A successful calculation has been made of the coercive force of material prepared by several earlier workers. A comparison of the new models with the older ones indicates a direction for experimental advance.

ACKNOWLEDGMENTS

It is a pleasure to acknowledge the close cooperation and encouragement of T. O. Paine, L. I. Mendelsohn, and F. E. Luborsky. Thanks are also due to W. H. Meiklejohn and J. C. Fisher for helpful suggestions.

PHYSICAL REVIEW VOLUME 100, NUMBER 4 NOVEMBER 15, 1955

Magnetic and Thermal Properties of $MnCl_2$ at Liquid Helium Temperatures. I. Magnetic Susceptibility*

R. B. Murray† and L. D. Roberts
Oak Ridge National Laboratory, Oak Ridge, Tennessee

(Received July 28, 1955)

Measurements of the magnetic susceptibility of polycrystalline and single-crystal samples of anhydrous $MnCl_2$ have been carried out from 1.1° to 4.2°K with an ac mutual-inductance bridge. The susceptibility was found to be essentially independent of an applied magnetic field up to 2400 oersteds throughout this region, and displayed anomalous behavior near 2°K indicating a magnetic ordering transition. In view of the observed susceptibility behavior this transition is interpreted as one of an antiferromagnetic nature, although the susceptibilities of both the single-crystal and polycrystalline samples were found to rise slowly with decreasing temperature below the transition region. This interpretation is supported by preliminary neutron diffraction studies below 2°K. A calculation of the magnetic anisotropy is in reasonable agreement with that observed at 4.2°K.

INTRODUCTION

ANHYDROUS $MnCl_2$ is a member of the series of iron-group anhydrous chlorides. The magnetic and thermal properties of these compounds have been previously investigated at a number of laboratories from liquid hydrogen temperatures to room temperature and above. An extensive study of the magnetic susceptibilities of the members of this group has been carried out by Starr, Bitter, and Kaufmann[1] (SBK); references to earlier work may be found in their paper. This series of compounds is of interest because of the high density of magnetic ions which leads to strong magnetic interactions, and hence to magnetic ordering transitions at relatively high temperatures. Many of these compounds are crystallographically isomorphous, having a hexagonal layer structure, so that their magnetic properties may be compared directly. Magnetic susceptibility measurements have shown well defined maxima in the susceptibilities of several compounds of this series, characteristic of an antiferromagnetic

* Reported at the New York meeting of the American Physical Society, January, 1955.

† Graduate Fellow of the Oak Ridge Institute of Nuclear Studies from the University of Tennessee. This work was included in a thesis submitted in partial fulfillment of the requirements for the degree of Doctor of Philosophy at the University of Tennessee.

[1] Starr, Bitter, and Kaufmann, Phys. Rev. 58, 977 (1940).